SCIENCE REQUIREMENTS DOCUMENT

FOAM

FOAM OPTICS AND MECHANICS

(The Melting of Aqueous Foams)

Douglas J. Durian _____ _____ September 21, 1998
Principal Investigator signature date
UCLA Physics & Astronomy
Los Angeles, CA 90095-1547
tel. 310-206-2645
fax. 310-206-5668
<durian@physics.ucla.edu>

Gregory A Zimmerli _____ _____ _____
Project Scientist signature date
NASA Lewis Research Center
tel. 216-433-6577
fax. 216-433-8050
<gregory.a.zimmerli@lerc.nasa.gov>

Susan M. Motil _____ _____ _____
Project Manager signature date
NASA Lewis Research Center
tel. 216-433-8589
fax. 216-433-8660
<susan.motil@lerc.nasa.gov>

TABLE OF CONTENTS

NOMENCLATURE

foam characteristics:

$\rho(d)$	bubble size distribution
D	average bubble diameter, $<\rho>$
ϕ	volume fraction of liquid
$1-\phi$	volume fraction of gas
T	age of foam
σ_f	surface tension of soap film made from surfactant solution
σ_s	liquid-vapor surface tension of surfactant solution
n_s	refractive index of surfactant solution
η_s	dynamic viscosity of surfactant solution
τ_d	duration of rearrangement events
δ	amplitude of thermal fluctuations

foam optics/multiple-light scattering:

λ	wavelength of laser light
k	wavenumber of laser light
ξ	coherence length of laser light
L	thickness of foam slab
l_s	photon scattering length
l^*	photon transport mean free path
l_a	photon absorption length
R_d	average diffuse boundary reflectivity
z_e	extrapolation length ratio, $(2/3)(1+R_d)/(1-R_d)$
T_b	ballistic transmission probability, $\exp(-L/l_s)$
T_d	diffuse transmission probability, $(1+z_e)/(L/l^*+2z_e)$
$g_2(\tau)$	normalized intensity autocorrelation function, $<I(0)I(\tau)>/<I>^2$
$g_1(\tau)$	normalized electric field autocorrelation function, $<E(0)E^*(\tau)>/<EE^*>$
Siegert relation, $g_2(\tau)=B+ßg_1(\tau)^2$	
B	baseline
ß	intercept
τ_o	DWS decay time scale for localized rearrangements
τ_s	DWS decay time scale for uniform shear deformation

foam mechanics/rheology and sample geometry:

α	cone angle
R	cone radius
I	cone + shaft moment of inertia
r	radial distance from rotation axis
L(r)	gap thickness at r
M	torque
F_z	total thrust
P(r)	pressure vs radial distance
P_a	ambient external pressure
N_1	first normal stress difference, $2F_z/\pi R^2$
N_2	second normal stress difference
θ	angular position
Ω	angular rotation speed, $d\theta/dt$
γ	shear strain, θ/α
$\dot{\gamma}$	shear strain rate, $d\gamma/dt$
$\Delta\gamma$	magnitude of step-strain
σ	shear stress, $3M/2\pi R^3\cos^2\alpha$
σ_y	yield stress
$\sigma(t)$	shear stress at time t after imposition of step-strain
$\sigma(\Omega)$	average shear stress at rotation speed Ω
η	dynamic viscosity of foam, $\sigma/\dot{\gamma}$
η_p	plastic viscosity of Bingham plastic
τ_p	Bingham plastic time scale, η_p/σ_y
G_o	static shear modulus
G(t)	shear relaxation modulus, $\sigma(t)/\Delta\gamma$
$G(t,\Omega)$	superposed shear relaxation modulus, $[\sigma(t)-\sigma(\Omega)]/\Delta\gamma$

ACRONYMS

DWS	diffusing-wave spectroscopy
DTS	diffuse-transmission spectroscopy
SDS	sodium dodecylsulfate
AOS	sodium C14-C16 alpha olefin sulfonate
CMC	critical micelle concentration
PEO	polyethylene oxide

0.0 EXECUTIVE SUMMARY

0.1 Objective

To exploit rheological and multiple-light scattering measurements in order to quantify and elucidate the unusual elastic character of foams in terms of their underlying microscopic structure and dynamics. Special interest is in determining how this elastic character vanishes, i.e. how the foam melts into a simple viscous liquid, as a function of both increasing liquid content and increasing shear strain rate.

0.2 Approach

The unusual elastic character of foams will be quantified macroscopically by measurement of the shear stress as a function of shear strain rate and of time following a step strain; such data will be analyzed in terms of a yield stress, shear moduli, and dynamical time scales. Microscopic information about bubble packing and rearrangement dynamics, from which these macroscopic non-Newtonian properties ultimately arise, will be obtained non-invasively by multiple-light scattering: diffuse-transmission spectroscopy (DTS) and diffusing-wave spectroscopy (DWS). Quantitative trends with materials parameters, most importantly average bubble size and liquid content, will be sought in order to elucidate the fundamental connection between the microscopic structure and dynamics and the macroscopic rheology.

0.3 Need For Microgravity

Aqueous foams are intrinsically nonequilibrium systems; with time, the gas and liquid components inexorably separate by some combination of coarsening (gas diffusion from smaller to larger bubbles), film rupture, and the gravitational drainage of liquid from in between gas bubbles. While coarsening is often slow and film rupture can be eliminated, gravitational drainage cannot be prevented on earth since it is not possible to density match gas and liquid; furthermore, the rate of drainage increases rapidly with liquid content. This fundamentally precludes the possibility of ground-based study of foams near the melting transition. Prolonged microgravity conditions are therefore required in order to eliminate drainage for experimental study of the intrinsic structure, dynamics, and rheology of foams with liquid content varying up to, and beyond, the melting transition.

0.4 Significance

The utility and fascination of foams derive largely from the surprising fact that they have a solid-like elastic character, in spite of being mostly gas with a few percent volume fraction of liquid, but can nevertheless flow under shear. The physical origin of such unusual rheology in terms of microscopic structure and dynamics is poorly understood and remains a subject of basic scientific interest to physicists, chemists, and chemical engineers. The proposed research promises important new insight into these issues, and could also have significant consequences for our understanding of flow in other dense randomly-packed systems such as emulsions, colloidal suspensions, slurries, bubbly liquids, and granular materials. Furthermore, all foam applications are empirically based and the proposed research may generate valuable fundamental guidance for the development of materials with more desirable rheology and stability characteristics.

1.0 INTRODUCTION AND BACKGROUND

1.1 Description and Review of Scientific Field

1.1.1 Aqueous Foam

Aqueous foam is a nonequilibrium collection of polydisperse gas bubbles packed in a smaller amount of water containing surfactants, or other surface-active macromolecules [1-7]. These preferentially adsorb at the gas-liquid interfaces and give rise to repulsive forces which prevent bubble coalescence. The typical bubble size can range from 10 μm to 1cm, and their minimum surface separation distance, i.e. the soap film thickness, can range from 10 Å to 1 μm. The volume fraction of liquid can be as small as 0.01%, such that the bubbles are nearly polyhedral, or as large as about 8% on earth, such that the bubbles appear slightly spherical. If made wetter, however, the liquid will rapidly drain under the influence of gravity; thus, the close-packing limit of about 35% liquid, where the bubbles are perfectly spherical, cannot be reached on earth. The following figure shows a schematic illustration of the key features of foam structure at various length scales; the photos show the actual bubble-scale structure in a single-surfactant foam (SDS in water), where the bubble size is 3 mm and where drainage and the influence of liquid content on bubble shape are evident, and in a commercial shaving foam (Gillette Foamy Regular), where the bubble size is 30 μm.

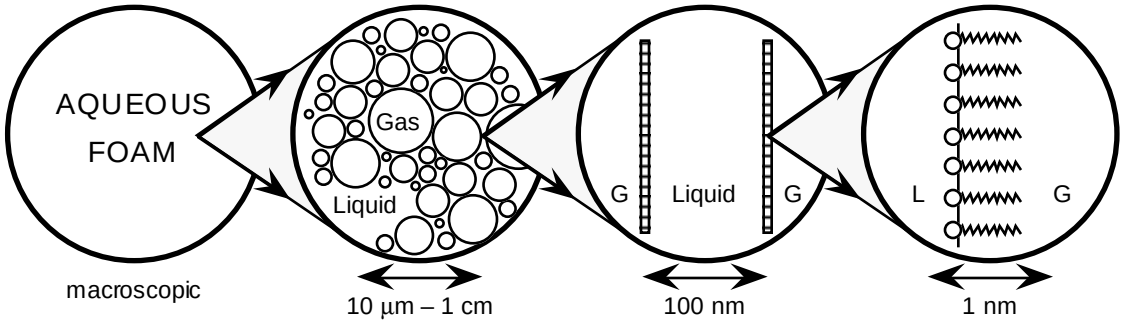

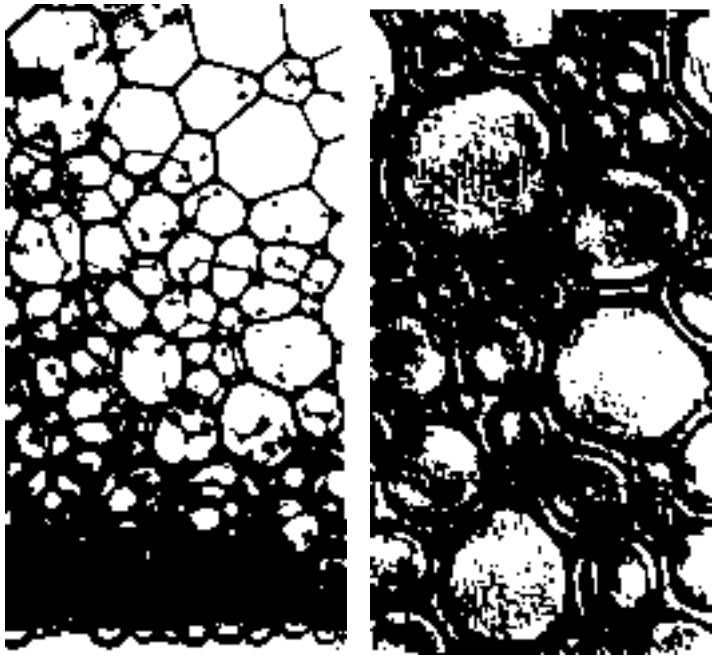

Hierarchy of structure and self-organization in aqueous foams.

Foams are thus highly organized materials that posses important structure on many length scales. Much is known about the behavior of surfactants at interfaces and about the behavior of soap films, including their relation to surfactant and liquid properties [8-13]; however, much less is known about the behavior at larger length scales. In particular, we do not know how to fully describe and extract the salient features of structure and dynamics at the bubble scale, or how to use this information to predict rheological behavior at the macroscopic scale. In no small part, this is because *the single-most important structural parameter –the liquid content– cannot be appreciably varied on earth*. The focus of the current ground-based research and the proposed Space Station experiments is to elucidate the collective behavior of the bubble-packing structure and its relation to the macroscopic rheology and stability properties of the bulk material.

1.1.2 Rheology

As a form of matter, foam is neither solid, liquid, nor vapor – yet it possesses the hallmark mechanical features of all three forms of matter. Under small applied shear forces, it can respond elastically, like a solid. Under large applied shear forces, it can flow and deform arbitrarily without breaking, like a liquid. Under pressure or temperature perturbations, it can proportionally change its volume, like a gas. This unusual rheological behavior in combination with low density and high interfacial area is the basis for our common fascination with everyday foams and for their utility in a wide variety of applications.

Efforts to measure and understand the quantitative rheology of foams are reviewed by other researchers in Refs. [1,14-16,3-5,17]. Widely cited experiments include those of Princen [18,19], Khan and Armstrong [20], and Mason and Weitz [21]; only those of Khan and Armstrong are on foams, the others are on emulsions. Since foams appear to exhibit a static shear modulus and to be shear-thinning above a yield stress, they are often described as Bingham plastics during flow and as a Kelvin solids under small deformations:

$$\sigma = \begin{cases} G_o\gamma + \eta_k\dot{\gamma} & \text{for } \gamma \ll 1 \quad \text{(Kelvin solid)} \\ \sigma_y + \eta_p\dot{\gamma} & \text{for } \dot{\gamma} = \text{const} \quad \text{(Bingham plastic)} \end{cases}. \tag{1}$$

The magnitude of the shear modulus and yield stress are set by surface tension, bubble size, and liquid content, while the plastic viscosity is set by interfacial- and film-level dissipation mechanisms involving surfactant transport and viscous flow.

The simple Kelvin-solid/Bingham-plastic picture provides valuable intuition, but is not necessarily correct –even qualitatively– for many reasons. First, it is difficult to ensure linear response due to neighbor-switching rearrangement of the bubbles induced by application of even very small shear; a truly linear regime may not exist. Second, the static and slow strain rate behavior can be severely affected by time evolution of the underlying packing structure via gas diffusion between bubbles (coarsening) or via drainage. Thus, for example, stress can relax after a step-strain and foam can creep under small applied stress; these features, as well as the complex dynamic shear modulus, are inconsistent with Eq.(1). Third, it is difficult to achieve a known, rheometric, velocity field due to plug-flow and wall-slip; this can invalidate analyses and render experiments irreproducible. Fourth, foams are disordered and polydisperse, and are hence difficult to characterize; this can lead to further irreproducibility. As an example, these effects combine to produce the following linear and flow rheology for a commercial shaving foam. Clearly, it is not a Kelvin solid, which behaves according to Eq.(1) as $G'(\omega)=Go$ and $G''(\omega)=\eta_k\omega$.

Clearly, also, it is not a Bingham plastic, since the stress does not approach a constant at low strain rates and since the viscosity does not approach a constant at high strain rates.

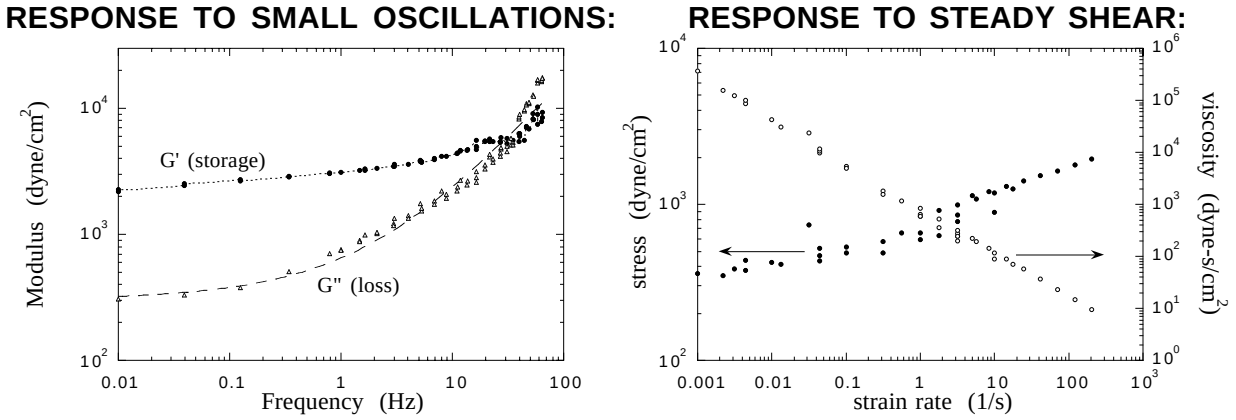

Rheology of Gillette Foamy Regular.

As a result of the above difficulties, accurate reproducible measurements of foam rheology and systematic trends with structural parameters are still in great need. The influence of surface tension σ_s and average bubble diameter D is relatively simple to measure and predict; namely, moduli are proportional to σ_s/D. The influence of dissipation mechanisms, e.g. liquid viscosity, by contrast is very difficult to predict; however, in the context of the Bingham plastic model, the only role is simply to set the value of the plastic viscosity, η_p, and hence the key dynamical time scale, $\tau_p=\eta_p/\sigma_s$. How to predict film-level flows and the value of this time scale are difficult fluids dynamics problem of current interest.

Note that surface tension, bubble size, and liquid viscosity all affect the basic moduli and time scales, but do not alter the general nature of the behavior. The influence of liquid content, however, is much more dramatic and much less understood. Most obviously, the liquid content dictates bubble shape, i.e. whether bubbles appear approximately polyhedral or spherical and whether more liquid resides in soap films or in Plateau borders and vertices. While photographs of a foam offer no clue as to chemical composition or bubble size, the liquid content is immediately evident from bubble shape. Therefore, *the volume fraction of liquid, ϕ, is the single most important parameter (a) in affecting foam structure and also (b) in producing the widest range of behavior as it is varied.* For example, as the foam becomes wetter, the ability to support shear decreases in accord with the complex shape of the bubbles until the shear modulus vanishes at the random close-packing volume fraction. As this melting transition is approached, the film-level flows, and hence dynamical time scales, must also vary significantly. Perhaps even more importantly, the stability of the packing structure with respect to neighbor-switching rearrangements must decrease too. These crucial dynamical issues have not been at all explored, either experimentally or theoretically, in any jammed system. Another important issue that has received no attention is the dependence of foam rheology on the evolution mechanisms and time scales to be discussed next.

1.1.3 Stability

Aqueous foams are continually-evolving systems far from equilibrium. With time, the gas and liquid portions inexorably separate by some combination of three basic mechanisms. First, if the quality or concentration of surfactants is too low, then adjacent bubbles can coalesce by rupture of the intervening soap film. This film-rupture mechanism can be eliminated easily by suitable choice surfactant and concentration. Second, the Laplace pressure difference between bubbles of different sizes causes gas to diffuse through the intervening soap film from the small to the larger bubble; thus, large bubbles grow and small bubbles shrink. This coarsening mechanism cannot be eliminated, but can be slowed by decreasing the surface tension of the interfaces and the solubility and diffusivity of the gas. Third, the unavoidably large density mismatch between gas and surfactant solution causes the bubbles to rise and the liquid to sink; as this proceeds, the soap films can become so thin as to rupture by thermal fluctuations. Gravitational drainage cannot be eliminated on earth; however, it can be slowed by decreasing the bubble size and by increasing the liquid viscosity and the gas content. Of these mechanisms, only coarsening represents a behavior intrinsic to all foams, since it cannot be eliminated even in principle. By contrast, rupture and drainage serve to complicate and mask intrinsic behavior and to prevent wide variation of key structural parameters such as liquid content.

Efforts to measure and understand drainage have been reviewed by other researchers for single soap films in Refs. [8,22] and for bulk foams in Ref. [23]. Efforts to measure and understand the coarsening of foams have been reviewed by other researchers in Refs. [2,5,24,25]. Widely cited experiments include those of Glazier [26], Knobler [27], Stavans [28], and the PI [29]; of these, only those of the PI are on three-dimensional foams. In all, part of the motivation was in topological constraints within the foam structure and their possible influence on the evolution process. For both two- and three-dimensional foams, the following picture of coarsening has emerged. The bubble size distribution, $\rho(d)$, evolves under the influence of coarsening to a stationary shape, such that $\rho(d/\langle d\rangle)$ is independent of time. Once this stationary distribution is reached, the average bubble diameter grows as a power-law with time. For dry foams, the growth exponent is 1/2; for wetter foams, the growth is not truly a power law but is often described as one with a smaller exponent; if the volume fraction of gas could be made negligible, the power-law would be 1/3 as in Ostwald ripening of binary alloys. The actual size distribution and growth law have not been predicted or observed systematically as a function of liquid content.

1.1.4 Structure

The bubble-packing structure of foams is difficult to describe, due to randomness and polydispersity. It is even more difficult to measure, since bulk foams are opaque. Due to the unavoidably large refractive index mismatch between the gas and liquid, incident light strongly reflects and refracts at the bubble interfaces and this multiple light scattering gives rise to their familiar white appearance. This restricts the use of light-based microscopies to surface structure and two-dimensional foams. Besides surface observation, other available probes of structure include electrical conductivity [30-32], external pressure [33], freeze fracture [34], penetration by optical fiber [35], and either MRI [36-38] or confocal microscopy [39] applied to small samples. Without exception, these are all either indirect and open to ambiguity of interpretation, invasive and therefore not suitable for *in-situ* and time-evolution studies, and/or too slow for all but the

most stable foams. The development of a superior means of quickly and noninvasively measuring the bubble-scale structure of foams would significantly advance our understanding of both foam rheology and foam stability.

1.2 PI's Research and Proposed Flight Experiment

The PI has written several review articles [40,41,6,42,43] summarizing both our knowledge of foam stability and rheology, as well as multiple light scattering and the particular contributions of his research.

Prior to NASA funding, the PI developed a superior means of quickly, noninvasively characterizing three-dimensional foams by use of multiple-light scattering [44]. This includes diffuse-transmission spectroscopy (DTS) as a probe of bubble-scale structure and diffusing-wave spectroscopy (DWS) as a probe of bubble-scale dynamics. Since foams are unavoidably opaque, these techniques can be applied quite generally. The PI also used these techniques to quantify, for the first time, the time-evolution of structure and bubble-rearrangement dynamics in a coarsening three-dimensional foam [29].

The general idea of the proposed flight experiment is to apply these techniques simultaneously with rheometric diagnostics on a series of coarsening foams with increasing liquid content. The PI has built a laboratory with start-up funds from UCLA and has carried out ground-based research toward this goal with funds from NASA. In brief, published accomplishments to date include the following:

- quantitative observation of localized stick-slip like rearrangement of bubbles during shear flow via DWS, establishing rearrangements as mechanism for large-scale deformation; discovery that flow does not affect coarsening [45]

- quantitative observation of thermal fluctuations of bubble interfaces via DWS and their direct relation to the macroscopic static shear modulus [46]

- thorough evaluation of the accuracy of the conventional diffusion theories used to analyze DTS [47] and DWS [48,49] data

- development of experimental means of characterizing the boundary conditions of the diffuse-photon concentration field (a key ingredient for the theories to be accurate) [50,51]

- extension of DTS and DWS theories to include effects of ballistic propagation and anisotropic scattering, plus thorough evaluation and demonstration of significant gains in accuracy [52-54]

- clarification of the role of the duration of rearrangements, τ_d, as an important time scale in foam rheology [55], direct observation via DWS that the bubble-scale deformation crosses over from discrete rearrangements to continuous shear as the strain rate exceeds this time scale [56]

- development of a new theoretical model that permits, for the first time, systematic study of trends in bubble-scale behavior and macroscopic time-dependent rheology as a function of liquid content, dimensionality, disorder, polydispersity, and evolution mechanisms [57,58]

Highlights of current, unpublished, work include the following:

- demonstration via step-strain superimposed upon steady flow that the rheology changes nature at the same time scale, τ_d, that bubble motion crosses over from discrete rearrangements to continuous simple shear

- development of simple means to produce high-quality foams of variable liquid content

- design of cone-and-plate sample cell for our commercial rheometer that permits simultaneous optical access for DWS and that has flush-mounted pressure transducers on the fixed plate for measurement of first and second normal stress differences

- study of forced drainage (in which liquid is continually introduced from above) as a means to tune liquid content; observation that it induces convection and size-segregation

Note that the individual optical and mechanical diagnostics (described in more detail next) and analysis tools have thus already been developed and applied, albeit individually rather than in a single coordinated experiment.

1.2.1 Video Microscopy: $\rho(d)$, τ_d

The most straightforward diagnostic of foam structure is to estimate the bubble size distribution, $\rho(d)$, from still-frames of bubbles at the surface where a bulk foam is pressed against an optically clear wall. This is also important for verifying that the sample is homogeneous, without any empty pockets filled with gas. From real-time video recordings, the sudden bubble-scale rearrangements can be directly observed near the surface and analyzed in terms of the key time scale, τ_d , the event duration.

1.2.2 Diffuse-Transmission Spectroscopy: l^*

In this diffusing-light spectroscopy, the probability T_d for incident photons to be diffusely transmitted is estimated from measuring the time-averaged transmitted intensity, $\langle I \rangle$, and normalizing by the intensity I_o of the incident light: $T_d=\langle I \rangle/I_o$ [44,47,59]. From ancillary knowledge/measurement of the extrapolation length ratio z_e and slab thickness L, the transport-mean free path l^* of the photons is then extracted using the diffusion-theory prediction $T_d=(1+z_e)/(L/l^*+2z_e)$. This provides a second measure of the foam structure since l^* is proportional to the average bubble diameter. The value of l^* is also a crucial ingredient needed for analysis of DWS data.

As an aside, recall that foam is opaque. Therefore, essentially no *unscattered* photons are transmitted though a bulk sample of foam since the thickness is much greater than the scattering length l_s. In other words, the ballistic transmission probability $T_b=\exp(-L/l_s)$, is much less than one and, in particular, is much less than the diffuse transmission probability T_d.

1.2.3 Diffusing-Wave Spectroscopy: $g_1(\tau)$

In this diffusing-light spectroscopy, temporal fluctuations in the diffusely transmitted light are characterized by real-time computation of the intensity autocorrelation function, $g_2(\tau)=<I(0)I(\tau)>/<I>^2$, using photon-counting and a digital correlator [60-62,44,63]. This is similar to traditional dynamic light scattering/photon-correlation spectroscopy, except that the detected photons have been multiply scattered, rather than singly by a selected scattering wavevector. The normalized field correlation function $g_1(\tau)=<E(0)E^*(\tau)>/<EE^*>$ is then extracted using the Siegert relation, $g_2(\tau)=1+ß g_1(\tau)^2$; this, in turn, is analyzed in terms of the nature and time scales of the bubble motion using the theory of DWS. For example, discrete rearrangements and uniform shear give contributions to $g_1(\tau)$ that decay roughly exponentially in $(L/l^*)^2$ times τ/τ_o and $(\tau/\tau_s)^2$, respectively, where τ_o is set by the size and frequency of the discrete rearrangements [29,45], and $\tau_s^{-1} = \dot{\gamma} k l^* / \sqrt{30}$ is set by the strain rate of the homogeneous deformation [64]. These features can be seen in the following DWS data taken for a foam in our homemade Couette cell at a series of increasing strain rates:

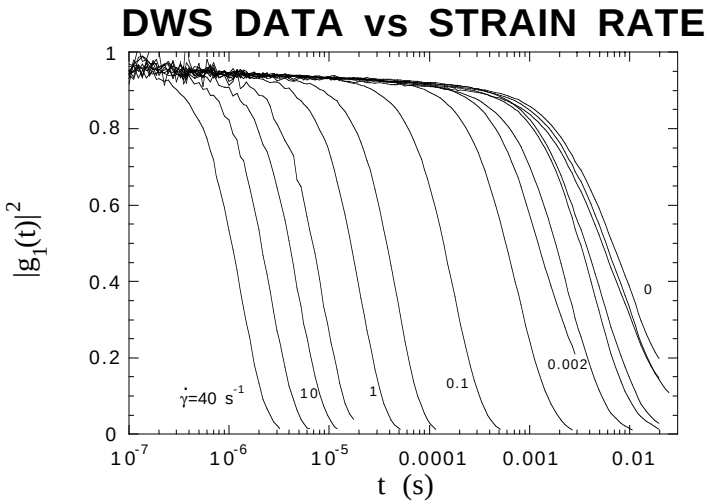

Microscopic dynamics probed by DWS during shear.

Note that digital correlators compute the average intensity as well as its temporal autocorrelation, and that therefore DWS measurements automatically yield DTS data (albeit at only one wavelength). The only extra requirement for doing DTS with a DWS set-up is to determine the normalization, which can be done by calibration or comparison with a known sample.

1.2.4 Stress Relaxation During Steady Shear: $\sigma(t, \dot{\gamma})$

In this rheological diagnostic, the first task is to measure the average shear stress $\sigma(\dot{\gamma})$ at the given angular rotation speed Ω or strain rate $\dot{\gamma}$. The next task is to superimpose a small amplitude step-strain $\Delta\gamma$ on top of the steady rotation and to measure the transient increase in stress $\sigma(t)$ and its relaxation back to the steady-state value $\sigma(\dot{\gamma})$; in other words, to measure the

generalized shear relaxation modulus $G(t, \dot{\gamma})=[\sigma(t)-\sigma(\dot{\gamma})]/\Delta\gamma$. This is to be checked for linearity by varying $\Delta\gamma$ and to be repeated for a range of rotation speeds, including zero where it reduces to the traditional shear relaxation modulus. This diagnostic is similar to the parallel superposition of small oscillations and steady flow used to study structured fluids such polymers and liquid crystals [65-70].

Plots of $\sigma(\dot{\gamma})$ and $\eta=\sigma(\dot{\gamma})/\dot{\gamma}$ vs $\dot{\gamma}$, and of $G(t, \dot{\gamma})$ vs t and $\dot{\gamma}$, serve to characterize the shear rheology of the foam without further analysis. Of course, however, other quantities may be extracted in the context of models such as the shear modulus, yield stress, yield strain, plastic viscosity, spectrum of relaxation times, etc. Example data obtained with our Paar-Physica UDS-200 rheometer are as follows:

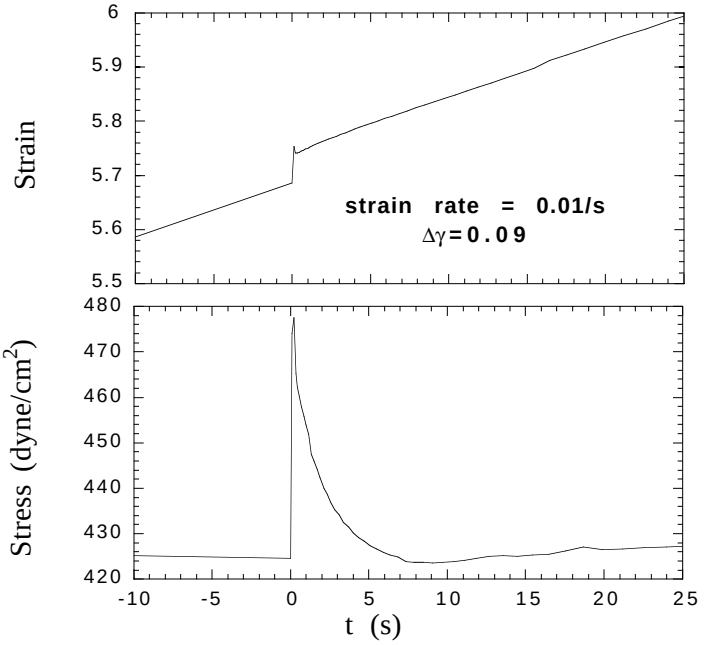

Relaxation after step-strain during steady shear

From this data we extract both the viscosity and the shear-relaxation modulus. This gives stress vs strain rate data shown earlier, and as well as the following picture of how the relaxation modulus decreases, and the foam becomes progressively more liquid-like, with increasing strain rate:

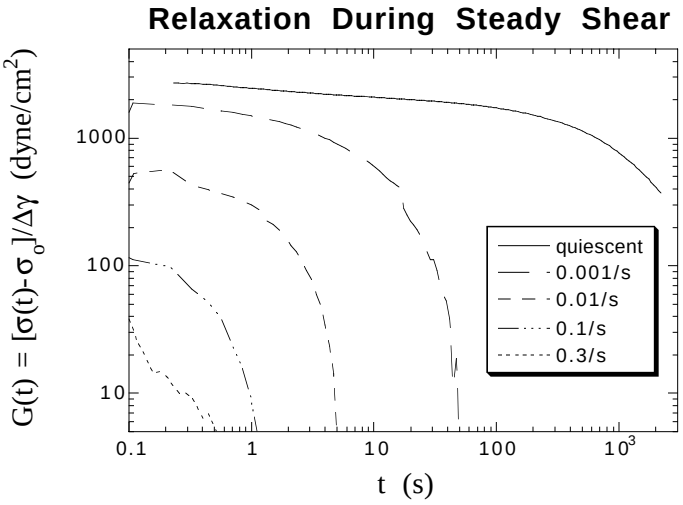

Melting vs strain rate

The melting transition as a function of increasing liquid content is expected to be rather different. According to simulation [58], the relaxation time actually increases while the static shear modulus goes to zero, as follows:

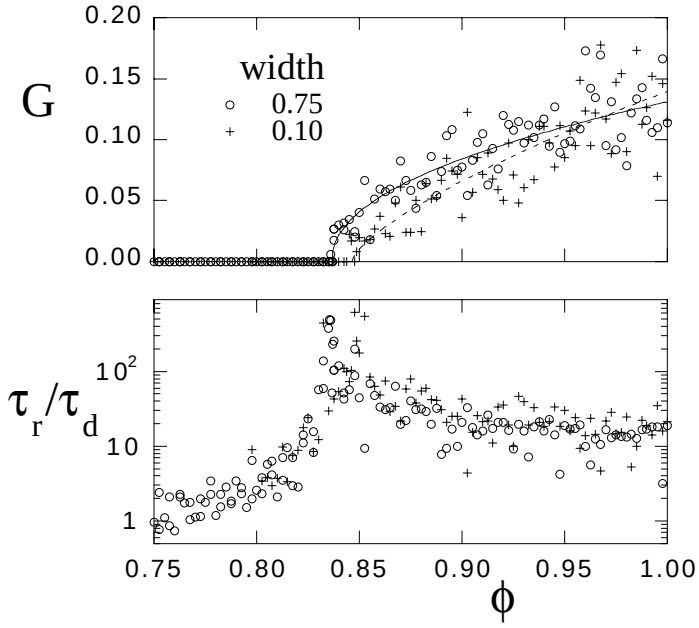

Melting vs liquid content

As an aside, recall that the unusual and interesting elastic features of foam rheology –including the role of rearrangements and interplay between rheology and coarsening– occur at small strain rates. Therefore, measurement of stress relaxation seems preferable to measurement of the complex dynamic shear modulus $G^*(\omega)$.

1.2.5 Normal Stress Differences: $N_1(t, \dot{\gamma})$ and $N_2(t, \dot{\gamma})$

In this rheological diagnostic, the first task is to measure the total thrust force F_z produced by the foam along the axis of the rotating cone of the sample cell; the first normal stress difference is then deduced as $N_1=2F_z/\pi R^2$. The second is to measure the pressure P(r) vs radial distance r using flush-mounted transducers; a second estimate of the first normal stress difference can then be deduced from $F_z=\int 2\pi r[P(r)-P_a]dr$, and the second normal stress difference can be found from $dP/d\ln r=N_1+2N_2$ [71]. These quantities are to be obtained as a function of strain rate, and of time following a step strain superimposed upon the steady flow, just as for the shear stress above.

Of the five diagnostics, only this has not yet been performed in the PI's lab. Normal forces arise as tightly-packed bubbles try to squeeze around one another during flow; therefore, they provide a more direct measure of the state of "jamming" of the system than do shear forces, since the latter also depend on viscous losses.

1.3 Experiment Objectives

The objective is to provide fundamental insight into the nature of foam rheology and stability in terms of the underlying bubble-scale structure and dynamics of the material. This is to be accomplished by application of the above five diagnostics to a series of foams of increasing liquid content as they slowly coarsen:

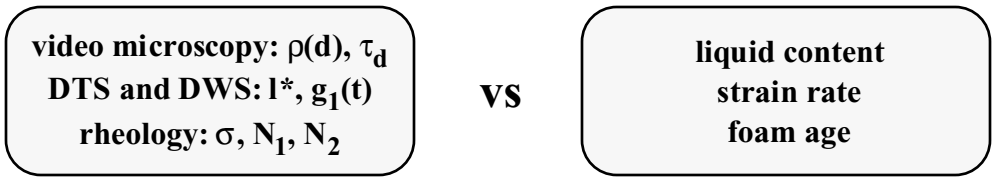

The rationale for systematic variation of liquid content and strain rate is described in detail above; in short, it is because these have the most pronounced influence on foam rheology and coarsening. The rationale for systematic measurement vs foam age is not just to observe and quantify coarsening, but also to observe variation of rheology with bubble size and, perhaps more importantly, to obtain a reproducible self-similar size distribution.

As discussed later, it is proposed to first perform limited-scope Glovebox experiments in which both the rheology diagnostics and the variation of strain rate are omitted.

1.4 Knowledge Gained, Value and Application

Reaching the above objectives will provide an unprecedentedly clear picture of the relation between the microscopic behavior and the macroscopic properties of foams. In particular, the state-of-the-art diagnostics applied in combination with microgravity conditions will sweep aside the difficulties traditionally encountered in obtaining accurate reproducible measurements of foam rheology and its systematic trends with structural parameters. The proposed space experiments will thus be able to provide unambiguous quantitative answers to the following open issues:

- characterization of complete time-dependent rheology of aqueous foams
- characterization of coarsening and its dependence on liquid content
- characterization of coarsening- and shear-induced bubble rearrangement dynamics
- dependence of complete time-dependent foam rheology on liquid content
- dependence of complete time-dependent foam rheology on bubble size
- dependence of bubble rearrangement dynamics on liquid content
- dependence of bubble rearrangement dynamics on strain rate
- role of shear-induced rearrangements as stress relaxation mechanism
- role of coarsening as stress relaxation mechanism
- interplay between coarsening and rheology
- nature of the melting transition at high liquid content
- nature of the melting crossover at high strain-rates
- dependence of foam behavior on surfactant, liquid, and gas properties

This will comprehensively reveal the basic phenomenology, for the first time, and will provide a definitive set of data for guiding and testing theories. Since we already understand much about the connection between molecular properties and the behavior of soap films and individual bubbles, this will fill in the missing link between bubble-scale and bulk behavior and will thus establish a fundamental understanding of foams ranging from molecular to macroscopic length scales.

While the motivation of the PI is in basic understanding, the knowledge obtained could provide rational guidance for improving the mechanical and stability properties in foam applications, some of which are listed in the appendix and all of which are based almost entirely on empirical trial and error.

Basic insight into aqueous foams should carry over well to nonaqueous foams, including the liquid foam precursors to rigid polymer foams and synthetic microcellular solids. Furthermore, it could also carry over to naturally occurring cellular materials such as plant and animal tissues, and the quest for man-made substitutes [72].

Looking further afield, foams are member of a broad class of disordered materials that exhibit features coming to be known as "jamming". This includes dense colloidal suspensions and emulsions, granular media and powders, molecular glasses, spin glasses, magnetic flux-line lattices in superconductors, and charge-density waves. All these systems consist of a large number strongly interacting units very far from equilibrium and for which k_BT is a small energy scale. When acted upon by only small external forces, the individual units are constrained by their interactions and geometry to remain in their given configuration, and are not free to explore phase space. Due to disorder, the static distribution of forces and stresses within the material can be highly heterogeneous at length scales ranging from the unit to the system size; this is not captured by continuum elastic descriptions, and could even invalidate their application. When jammed systems are acted upon by sufficiently large external forces, by contrast, the units can acquire enough energy to rearrange and thus to flow and deform and explore configuration space. Due to disorder and geometrical constraints, the dynamics are highly nonlinear and collective –i.e. cannot be understood in terms of unit-unit interactions; again, this gives rise to complex heterogeneous behaviors at many length and time scales that are not captured by a continuum

description. Study of the microscopic statics and dynamics of jamming is at the very forefront of modern condensed matter physics and nonlinear science. The proposed space experiments on foams could provide crucial insight into jamming in general, for at least three reasons. (a) Foams are perhaps the simplest. For example, emulsions are essentially foams where the bubbles also have inertia and internal viscosity, and can respond more readily to k_BT; colloidal suspensions are essentially foams where the bubbles have fixed shapes, inertia, long-ranged interactions, and can respond more readily to k_BT; granular media are essentially foams where the bubbles have irregular fixed shapes, inertia, and static tangential forces. (b) Of all these systems, our experimental ability to simultaneously probe the microscopic and macroscopic behaviors is perhaps the greatest for foams. (c) Of all these systems, our theoretical understanding of microscopic physics of the individual units and their pairwise interactions –both storage and loss– is perhaps the greatest for foams. Thus, study of foams should considerably advance our understanding of the phenomenology and theory for jamming in disordered highly-constrained systems.

2.0 JUSTIFICATION FOR EXTENDED MICROGRAVITY ENVIRONMENT

2.1 Limitations of Ground-Based Testing

Since the rate of drainage in foams increases with liquid content, the volume fraction of liquid accessible on earth is restricted to a very narrow range, below about 8%, where the foam is still relatively dry with nearly polyhedral bubbles. Therefore the dramatic changes in foam structure, bubble dynamics, coarsening, and rheology that are expected on approach to the melting point at about 36% liquid cannot be studied by ground-based experiments. Furthermore, the intrinsically large mass density difference between gas and liquid precludes broader variation of liquid content simply by clever choice of material, as in the density matching of colloids or binary-liquid mixtures.

One possibility to extend the range of accessible volume fractions on earth is to establish a steady state where the liquid which drains out the bottom is replaced by a continuous rain of liquid from above. However, this is not satisfactory for several reasons. (a) The liquid preferentially travels down through Plateau borders such that the bubble shapes are different from what they would be in zero gravity but with the same average liquid content; this alters both coarsening and rheology. (b) We find that the downward flow of liquid can induce stratified convective rolls as well as size segregation of bubbles in polydisperse foams [73]; this alters both coarsening and rheology. (c) This "forced/steady-drainage" could be implemented in a Couette rheology geometry, but not in the cone-plate system.

Another possibility to extend the range of accessible volume fractions on earth is to tumble the entire system or otherwise provide continuous mixing. However, this is not satisfactory for several reasons. (a) Same as reason (a) above. (b) Uniaxial spinning may merely replace vertical gravitational drainage with radial centrifugal drainage. Under more complex tumbling or stirring there is no guarantee that the volume fraction would be homogeneous throughout the system unless there is also rapid convection of bubbles; this would alter coarsening and rheology. (c) Even with rapid convection, our experience is that the system still becomes inhomogeneous,

especially at high liquid content. Perhaps the single most important limitation is that: (d) Steady tumbling or stirring cannot be implemented simultaneously with rheological diagnostics. Nevertheless, it may offer some overlap with low-g DWS data for fairly dry foams, in the 5-20% liquid content range.

In short, progress can be made on earth but only in carrying out the optical and mechanical diagnostics for relatively dry foams far from the melting point. However, even then, drainage is not absent and this (a) raises ambiguities as to its relevance and (b) prevents the long duration runs needed to obtain reproducible bubble-size distributions and to fully characterize coarsening.

2.2 Limitations of Drop Towers, Aircraft, and Sounding Rockets

The minimum time required for the structure of a freshly prepared foam to coarsen into a reproducible distribution of bubbles sizes ranges from tens of minutes to a few hours. After that, several hours to several days are needed to allow the coarsening process to proceed appreciably. Furthermore, the DWS and rheology diagnostics require tens of minutes at each point in the foam's lifetime. Thus, only DTS and video microscopy could be usefully performed in drop towers, aircraft, or sounding rockets; however, even then, the results would be ambiguous because the bubble size distribution would not be reproducible.

2.3 Need for Accommodation in Space Shuttle or Space Station

We may draw the following conclusions from the above two sections, 2.1-2.2:

Microgravity conditions are the only viable alternative to eliminate drainage and hence to enable study of the dramatic changes in foam structure, bubble dynamics, coarsening, and rheology that occur as the liquid content is increased toward the melting point.

Experiment durations of several hours to several days are needed in order to obtain reproducible self-similar bubble size distributions via the coarsening process, to observe appreciable self-similar coarsening of the foam, and in order to perform DWS and rheology diagnostics.

The requirement for prolonged microgravity conditions can be met only by accommodation in the Space Shuttle or Space Station.

2.4 Limitations of Modeling Approaches

Our understanding of foam structure, film- and bubble-scale dynamics, coarsening, rheology, as well as their detailed interplay, is not sufficiently advanced to quantitatively predict the experimental results sought aboard the Space Station. The data to be obtained will be able to guide development of improved theories, but no theory cannot replace experiment. The various modeling approaches and their limitations are briefly described below.

2.4.1 Analytic Approaches

The static rheology of perfectly dry, two-dimensional, periodic foams was worked out by Princen [74,75] and Prud'homme [76]. The key to this work is the fact that in 2D, the equilibrium structure of a periodic dry foam is simply a honeycomb network of perfect hexagonal bubbles. When subjected to shear, the hexagons distort nonaffinely and produce restoring and normal forces due to the increased interfacial area. This approach gives predictions for the static shear modulus and the yield strain, though only the former is qualitatively correct for real foams.

2.4.2 Film + Plateau Border Models

Real foams are three-dimensional, disordered, contain a finite volume fraction of liquid, and dissipate energy during flow; none of this is accounted for in the Princen-Prud'homme model. To incorporate disorder requires that analytic calculations be abandoned in favor of numerical work and computer simulation. Important steps in this direction were pioneered by Weaire and co-workers [77-81]. Besides explicitly incorporating disorder, this body of work further extends the Princen-Prud'homme model to finite volume fractions by decorating each Plateau border with a small amount of liquid. However, this approach fails at moderate-to-high liquid content, $\phi>0.10$, so that the behavior near the 2D melting point, $\phi\approx0.16$, cannot be fully explored. Furthermore, it is restricted to two-dimensions because there the curved interfaces are circular and specified by only curvature and endpoints.

2.4.3 Surface Evolver

Important progress have been made in the last several years in making the leap to three-dimensional foams. The key was the development by Brakke of the "Surface Evolver" program to compute minimal surfaces for the given topology and boundary constraints [82]. For example, Weaire and Phelan have used it to discover a unit cell for a periodic 3D foam structure which has less interfacial area than the Kelvin cell [83], previously conjectured to be the smallest. It has also been used by Reinelt and Kraynik to investigate large deformation and yielding of the Kelvin structure [84], as well as linear response of more exotic periodic structures [85]; they are now incorporating finite volume fractions of liquid and are producing disordered unit cells of roughly $5\times5\times5$ bubbles [86]. The limitations of this approach in terms of how close the melting point can be approached, and of how well a small disordered unit cell can model a bulk foam, remain to be explored.

The Film + Plateau border and Surface Evolver approaches are important because they are able to account for, at least to some extent, the effects of disorder and finite liquid content. However, by their very nature, they cannot incorporate film-level dissipation mechanisms and are hence limited to strictly quasi-static deformation at zero strain rate. Thus, they cannot be used to study the dynamics of bubble-scale rearrangements, or to test predictions for Bingham plastic flows and Kelvin solid oscillations; they can only model static elastic response and the onset of yielding.

2.4.4 Vertex Model

The first attempt to incorporate disorder and dissipation simultaneously was made in the vertex model of Kawasaki [87-89]. In this approach, the foam structure is simplified to be two-

dimensional, to have zero liquid content, and to have straight, uncurved, soap films; it can thus be described entirely by the positions of the vertices at which three films meet. If the angle between adjacent films is not 120º, then the surface tension force on the vertex is nonzero and it will move. Coupled equations of motion for the vertex locations can then be generated by balancing surface tension forces against dissipation forces, assumed to be of a particular form from studies of viscous flow within and near dry Plateau borders [90-92]. This allows computer simulation of flow at finite strain rates. However, since it operates on vertices alone, this approach is restricted to 2-dimensional foams with zero liquid content.

2.4.5 Bubble Model

The ***only*** approach that permits simulation of foam behavior at arbitrary liquid content, dimensionality, disorder, *and* strain rate, is the so-called "bubble model" developed by the PI [57,58]. Here, the foam structure is simplified such that the gas bubbles are described only by their position and radius. Storage and loss mechanisms are then estimated in terms of these quantities, and used to generate coupled equations of motion that can be solved numerically for the desired flow conditions. In particular, the increase in energy when two isolated bubbles are brought into contact is modeled as a spring force, and the dissipative forces between sliding bubbles due to film-level mechanisms is modeled as proportional to velocity difference. The resulting equation of motion depends only on a single force constant, representing effects of surface tension and bubble geometry, and a single time constant, giving the duration of rearrangement events and representing combined effects of all loss mechanisms. This approach has been used by the PI to study static elasticity and stress relaxation upon approach to the melting transition, and to study stress and bubble-rearrangement dynamics during uniform flow at finite rates. It has also been used to investigate force chains and anomalous dissipation in the linear regime [93] as well as rearrangement dynamics upon approach to the melting transition [94]. It is worth emphasizing that the bubble model is the ***only*** approach which permits study of the collective motion of the disordered bubble-packing configuration ***during*** rearrangement.

The obvious limitation of the bubble model is that is does not accurately represent the true microstructure and dissipation mechanisms. However, subtle corrections to strict harmonicity in the repulsive forces [95] are easily incorporated [96-98]. Also it is thought [99] possible to include more realistic loss mechanisms as they are currently understood from study of films [8,90-92,22,17] as well as droplets and dilute emulsions [100-105]. While, in this sense, the bubble model could conceivably provide a means of building up foam rheology through systematic approximation of actual film-level phenomena, this is not the spirit in which it was put forth. Rather, the spirit is to recognize and take advantage of the separation of length scales that exists between the bubble-packing and film levels, similar to how fluid dynamics starts with the Navier-Stokes equation rather than with a molecular model of liquid structure.

2.4.6 State of the Art

In summary of 2.4.1–2.4.5, exciting progress has been made in recent years in incorporating the effects of disorder, dimensionality, dissipation, and liquid content into a coherent theory. However, no single approach can handle all aspects at once. Furthermore, no attempt has yet been made to include time evolution simultaneously with rheology. Thus, only limited theoretical contact could currently be made with the proposed space experiments, and even then

only through use of more than one approach. The rigor of Surface Evolver for statics and the flexibility of the Bubble Model for dynamics and time evolution will no doubt prove useful for future analyses.

2.4.7 Emulsion-Foam Analogies

Emulsions consist of oil droplets suspended in water, or vice-versa, stabilized by surfactants, They are similar in appearance to foams, but with the potential advantage that the two liquid components could in principle be density matched in order to prevent drainage at low droplet fractions. Perhaps, therefore, much could be inferred about foam rheology from ground-based study of emulsions. Unfortunately, however, the quantitative analogy between the two systems is limited, and even where they are similar foams can offer distinct advantages:

- Droplet inertia is important in emulsions, but not in foams; so they can behave very differently at finite strain rates and during droplet rearrangement.

- Droplets are incompressible in emulsions, but not in foams; so they can behave very differently under large deformation, during rearrangement, and at finite strain rates.

- Coarsening is slow in emulsions, and may be stopped altogether through insoluble additives; therefore, it cannot be studied on reasonable time scales.

- Coarsening-induced rearrangements are an important stress-relaxation mechanisms in foams, but not in emulsions; therefore, the interplay between rheology and stability that is crucial in foams cannot be studied through emulsions.

- Coarsening cannot be used practically to achieve a reproducible self-similar distribution of droplet sizes in emulsions, as it can for foams. Therefore, (a) the droplet size distributions of the two systems will differ, producing differences in behavior and ambiguities in quantitative comparisons, and (b) only monodisperse emulsions can be reproducibly prepared.

- Monodisperse emulsions can be prepared in a disordered state, but the nature of the disorder is different from that in disordered polydisperse foams. Furthermore, disordered monodisperse systems tend to crystallize when subjected to shear.

- The volume fraction of the continuous phase can be made much smaller, i.e. the droplets can be much more compressed, in foams. Furthermore, compressed emulsions tend to break (fracture) when subjected to large deformation.

In short, emulsions may provide useful model systems for certain aspects of foams –particularly linear static rheology– but gross differences exist and quantitative comparison of similarities is fraught with ambiguity.

3.0 EXPERIMENTAL PLAN

3.1 Flight Experiment Procedure

The ultimate space experiments are conceived to proceed as follows. First the given foam is flowed into the sample cell through a loading port and checked visually to ensure that no open pockets of gas remain within the measuring volume. The foam is then allowed to coarsen for a specified period of time, and this process is monitored by video microscopy as well as the two diffusing-light spectroscopies. Next a series of rheological diagnostics are performed vs strain rate, synchronized with DWS measurement of the shear-induced dynamics. After the strain rate sweep, the foam is allowed to coarsen until the average bubble size has grown noticeably, and the measurement cycle repeats. After sufficient coarsening, the cell is cleaned out and the entire procedure is repeated for a foam with different liquid content.

The required experimental apparatus is depicted schematically in the following figure.

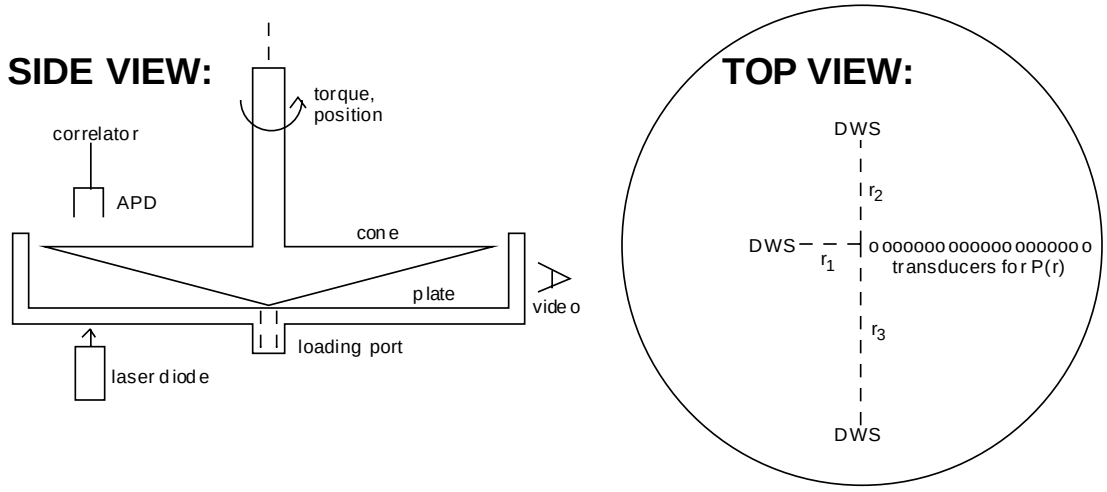

The ultimate flight experiment

Foam will fill the entire space between the rotating cone and the fixed plate and sidewall; the inner surfaces of the cone and plate will be roughened to achieve a no-slip boundary condition, and the sidewall will be smooth to allow the foam to slip and to allow video access. For clarity, only one DWS setup of avalanche photodiode + correlator is shown, on the left in transmission geometry. It is desirable to perform DWS in transmission at several radial positions, and hence at several different foam thicknesses, and to perform DWS in backscattering at the largest radial position where the foam is the thickest. The thickness is changed in order to probe behavior at different length and time scales, just as the scattering wavevector is changed in traditional dynamic-light scattering. Note that this cannot be done with a Couette cell, where foam fills the gap between concentric cylinders. The cone-and-plate geometry is further preferred because it is more compact, and also easier to take apart for cleaning and changing samples.

Foam samples will be made by standard procedures. The PI currently uses aqueous solutions of anionic surfactants such as sodium C14-C16 alpha olefin sulfonate (AOS) or of sodium dodecyl sulfate (SDS) at concentrations just above the critical micelle concentration (CMC). To produce foam, the PI currently employs a turbulent mixing scheme in which gas plus solution are metered at large Reynolds number through a small orifice and a long tube, as done in applications requiring large volumes of foam [106-109]. This method is useful in ground-based studies because the surfactant solution, gas, and liquid content can all be controlled. However, the production apparatus is somewhat unwieldy and requires skill to use. For the ultimate flight experiments, it would be desirable to switch to the aerosol method, employed for example in producing shaving

cream [110]; this would require outside contracts for delivery of one miniature can per desired surfactant solution and liquid volume fraction. A further advantage is that, since the aerosol method utilizes a phase separation process, the initial bubble size distribution is more nearly self-similar and should thus required less time to reach the scaling state.

3.2 Flight Experiment Test Matrix

Microgravity conditions will permit, for the first time, systematic study of foam rheology and stability as a function of liquid content without the deleterious effects of gravitational drainage. For a given surfactant solution, foams are therefore to be produced with a range of liquid contents extending over the full range of behavior, from the dry up to and just beyond the melting point near 37% liquid. To observe coarsening and to exploit it for systematic study of rheology vs bubble size, each foam sample is to be left in the rheology cell and studied periodically for a duration of up to one day. An example matrix of foams to be studied vs day in space is:

day	surfactant solution	liquid fractions
1-12	#1: AOS	ϕ=0.05, 0.10, 0.15,
13-24	#2: AOS+cosurfactant	0.20, 0.23, 0.27,
25-36	#3: AOS+thickening agent	0.30, 0.32, 0.34,
37-48	#4: AOS+polymer	0.36, 0.38, and 0.40

sample schedule

For each solution, foams will be produced with liquid fractions varying throughout the full range $0.05<\phi<0.40$. The surfactant solutions differ from one another in terms of film-level behavior, all starting from the same base solution, #1, of AOS. Presuming there is time, #2 will have an additive causing the films to be rigid rather than mobile, #3 will have an additive causing the solution viscosity to increase by a factor of ten, and #4 will have a polymer additive causing the solution to be viscoelastic at a time scale competing with the rearrangement duration. The full range of liquid fractions is to be examined for each solution.

For each foam sample, there are two sets of measuring activities that are to be repeated one after the other for a total duration of approximately one day. The first is the coarsening phase, during which the foam is quiescent, and the second is the rheology phase, during which the foam is subjected to a sweep of strain rates. The rheology phase requires a fixed length of time independent of foam age, say ten minutes, and the coarsening phase occupies all the time between successive rheology phases. An example test matrix of diagnostics vs time for a given sample is:

Foam Age (min)	Astronaut Activity	Measuring Phase
-15<T<0	set-up apparatus	
	set-up foam maker	
	save sample for ϕ determination	
T=0	flow foam into cell and	
	start data-taking software	
0-20	none	coarsening
20-30	none	rheology
	none	coarsening
50-60	none	rheology
	none	coarsening
100-110	none	rheology
	none	coarsening
200-210	none	rheology
	none	coarsening
500-510	none	rheology
	none	coarsening
1000-1010	none	rheology
1010-1025	clean cell, shut down	

test matrix for each sample

Note that, because of power-law growth, the rheology phases commence at foam ages that grow by successive factors of two. The exact times and number of repetitions are, of course, elastic and will be chosen closer to flight-time to maximize the science return for each specific foam sample. However, the total run duration per sample is not expected to exceed one day. The matrix of diagnostics to be performed during alternate coarsening and rheology periods is:

	Coarsening Phase	Rheology Phase
Microscopy	one 10 minute recording	none
DWS+DTS	successive 0.1T duration runs	synchronize runs with strainrates
Rheological	none	0.003, 0.01, 0.03, 0.1, 0.3, 1 s^{-1}
		average torque and P(r), and their
		relaxation with time after
		superimposed step-strain of 1%

diagnostic schedule per measuring phase

3.3 Postflight Data Handling and Analysis

Back on earth, the foam samples loaded into sealed containers just prior to T=0 will be weighted to determine/verify the liquid volume fraction.

Standard techniques will be used to analyze all other raw data. As described in previous sections, (a) video microscopy recordings will be used to estimate the bubble size distribution as well as the frequency and duration of rearrangement events; (b) DWS and DTS data will be used to

extract the field correlation function and the transport mean free path of light, and interpreted in terms of bubble-scale structure and dynamics; (c) rheological torque and pressure data will be expressed in terms of stress vs strainrate and of the generalized shear stress and normal stress difference relaxation moduli. All scientific conclusions will be based on trends and comparisons with the resulting dataset.

3.4 Ground Test Plan

It is crucial that the actual flight apparatus, and/or an exact replica, be thoroughly calibrated and tested with dry foams, where drainage is slow. The above test matrices should be executed and varied to as large an extent as possible in order to (a) determine potential flaws and idiosyncrasies; (b) allow minor design improvement; (c) provide a baseline for comparison with flight data; (d) finalize surfactant formulations; (e) finalize test matrices; (f) implement data analysis tools so that unanticipated behavior in space can be identified and used to alter the test matrices.

3.5 Mathematical Modeling

Application of the Bubble Model for modeling three-dimensional foams with a range of repulsion laws, dissipation mechanisms, liquid contents, and strain rates, would greatly assist in (a) anticipating behavior of the flight experiments on very wet foams, and (b) in building intuition with which to extract the fullest possible scientific meaning from the ultimate dataset.

Application of Surface Evolver for creating realistic three-dimensional foam structures with a range of liquid contents would also be useful for (a) providing a baseline with which to compare static rheology results from both experiment and the Bubble Model, and (b) providing input to optical ray-tracing software with which to model the characteristic optical length scales ls and l* upon which DWS and DTS are based.

These modeling tasks require significant human and computational resources beyond those available to the PI.

3.6 Limited-Scope Glovebox Experiments

Prior to the ultimate flight experiments described above, it is both desirable and prudent to perform limited-objective experiments of less complexity. In particular, before attempting rheological diagnostics it is crucial to first verify that (a) high-quality homogeneous foam samples can be produced with high liquid content, and that (b) these behave as expected with regards to handling, wall effects, and aging. For example, we must guard against the following possibilities:

- failure of foam-making procedures due to microgravity
- change of volume fraction or homogeneity upon loading into sample cell
- leakage of liquid component out from open sample cell due to wetting effects
- segregation of liquid and gas components due to wetting effects
- failure of no-slip boundary condition due to wetting effects

None of these can be checked on earth. Furthermore, in order to help finalize the ultimate test matrices, it would be useful to characterize wet foams in terms of their bubble-scale structure, rearrangement dynamics, and time evolution. This would also be of great scientific interest.

Fortunately all of these issues can be addressed with rather simple Glovebox experiments, as follows. To test production, handling, and wetting-induced leakage, two identical foam samples are to be flowed into rectangular sample cells:

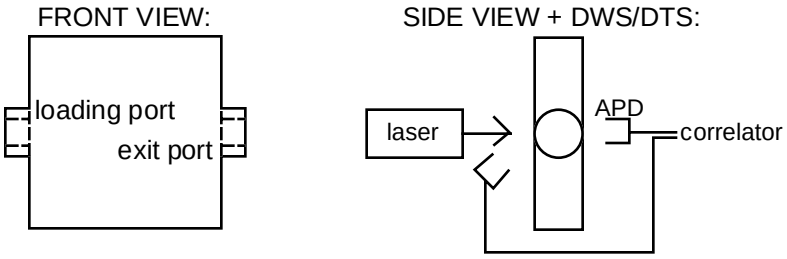

Glovebox experiment

These are to be made of the same non-wetting material as the cone and plate, but to be of sufficient optical quality to permit video microscopy. One sample will be completely sealed by screwcap, and the other will be closed with a screwcap of the nonwetting material but with a slot milled into it of the same width as the gap between the cone and sidewall of the future rheology cell. Both will be subjected to video and diffusing-light diagnostics vs age, and the sealed sample will be returned to earth for liquid volume fraction determination by weighing. Several such pairs of samples can be made at different volume fractions, and manually transferred back and forth between separate video and DWS stations. For each, an example test matrix is:

Foam Age (min)	Astronaut Activity
-15<T<0	set-up apparatus
	set-up foam maker
T=0	flow foam into cells and close
5-10	video on #1, DWS on #2
10-15	video on #2, DWS on #1
25-30	video on #1, DWS on #2
30-35	video on #2, DWS on #1
90-100	video on #1, DWS on #2
100-110	video on #2, DWS on #1
290-300	video on #1, DWS on #2
300-310	video on #2, DWS on #1
310-320	store sealed sample, shut down

glovebox test matrix

This is to be supplemented with visual inspection for leakage and bubble/liquid segregation. Another cell is to be filled in advance with an aqueous suspension of polystyrene spheres and brought along for calibration. Note that there would also be considerable science return for such a series of experiments, especially regarding the influence of liquid content on coarsening.

Elimination of wall-slip can be verified by visual inspection of the flow pattern at the open edge of the following shear cell composed of two disks on a spindle:

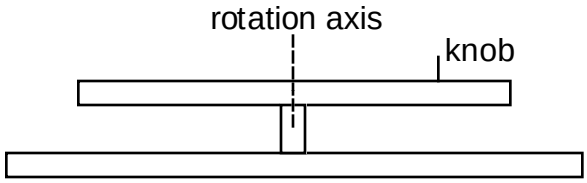

Glovebox shear cell

Both disks are to be made of nonwetting material and to be roughened on their interior surfaces, exactly as for the future cone and plate rheology cell. After flowing foam into the gap out to the radius of the upper disk, simply scratch a smaller vertical line across the open foam edge, hold the lower disk, and slightly rotate the upper disk while observing the deformation of the scratch mark. This experiment could also be performed aboard aircraft in free-fall trajectories.

4.0 EXPERIMENTAL REQUIREMENTS

4.1 Science Requirements Summary

To meet the science goals requires that four separate tasks be accomplished in coordination:

- foam production with variable liquid content
- video microscopy: bubble size distribution and rearrangement duration
- diffusing-light spectroscopy: $g_1(\tau)$ and l* respectively from DWS and DTS
- rheology: σ, N_1, N_2 vs strainrate and time following superposed step-strain

The test matrices, as well as measurement and analysis procedures, were discussed above. In order to obtain meaningful data, the instrumentation must meet the requirements discussed below.

4.2 Sample Requirements

Apparatus is required to produce foam samples of variable liquid content and chemical composition, according to the above test matrices, in sufficient quantity to fill the sample cells (roughly 100 ml). The liquid content shall be varied from 5 to 40%, and be known to an accuracy of better than 0.2%, for a sequence of foams with identical chemical composition. The average bubble diameter shall be between 10 and 30 μm upon production, with no inhomogeneities or bubbles larger than 3 times the average. The bubble size distribution and liquid content shall be constant throughout the sample volume.

The precise chemical composition of the base aqueous surfactant solution and gas is not critical, but must be known and be constant for a given volume fraction sequence. The water shall be distilled and deionized, the surfactants and additives shall be of high purity, and the gas shall be of a single molecular species. Modifiers of viscosity and film properties shall be added to the

same base solution, if possible. All surfactant solutions shall be made available for ground-based characterization of viscosity, surface tension, film properties, conductivity/screening length, etc.

Chemical compositions shall be finalized according to the results of ground based studies, the limited-scope Glovebox experiments, and the production method (aerosol is preferred over turbulent mixing).

4.3 Sample Cell & Test Chamber Requirements

4.3.1 General

The sample cell into which foams are loaded shall accommodate simultaneous video microscopy, diffusing-light spectroscopy, and rheological measurements. It shall permit foams to be loaded without introduction of gas pockets and other such structural or compositional changes or inhomogeneities. It shall permit rapid disassembly for discarding samples and for cleaning.

4.3.2 Temperature Measurement and Control

The set temperature of the test chamber shall be maintained near room temperature, anywhere in the range 20–30ºC. While the value is not critical, it shall be held constant to within ±0.2ºC, be measured to a similar accuracy, and be the same for all foams samples.

4.3.3 Pressure Measurement and Control

Similar to temperature, the pressure in the test chamber shall be maintained near 1 ATM, be held constant to within ±0.01 ATM, be measured to a similar accuracy, and be the same for all foam samples. Since samples cannot be sealed, evaporation shall be discouraged by maintaining appropriate humidity.

N.B. The rationale for holding temperature and pressure at a fixed constant for all samples is as follows. First, since foams are mainly gas, they can expand or shrink in response to pressure and temperature changes in rough accord with the ideal gas law, $V \propto T/P$. Second, liquid viscosity and rate of coarsening both vary appreciably with temperature.

4.4 Rheology Requirements

Requirements for the three diagnostic systems are now discussed, staring with the most global and stringent (rheology) and ending with the most lenient and easy to accommodate (microscopy). For all three, data must be time-stamped according to foam age.

The sample cell shall provide uniform shear deformation throughout the sample; this can be accomplished with either the cone-and-plate or the concentric-cylinder Couette-type geometries. The cone-and-plate is strongly preferred for the reasons cited earlier (more compact, easier to load and to clean, permits both diffusing-light spectroscopies and video microscopy to be employed). However, since rheology is important in so many areas of fluid physics, the

apparatus should be designed such that other researchers may incorporate their own measurement geometries and ancillary optical probes.

With a general-purpose design, the dimensions of the sample cell are not critical to specify in advance. General requirements are that the radius and cone-angle be large enough to accommodate bulk foam samples and several optical probes, but small and light enough that the cone+shaft moment of inertia not limit performance. The following should delimit the useful range of cell dimensions:

- cone angle, α: 0.1–0.2 radians
- cone & plate radius, R: 5–10 cm

The gap at distance r from the rotation axis, $L(r)=r\tan\alpha$, would then vary from zero at r=0 to a maximum of 0.5–2 cm at r=R. The cone and plate material shall be nonwetting, their inner surfaces shall be roughened in order to provide a no-slip condition, and their outer surfaces shall be of optical quality. The sidewall shall be nonwetting, and be optical-quality smooth on inner and outer surfaces both in order to provide a slip condition and to permit access for video microscopy.

Assuming a cone-plate geometry of typical size, the following table illustrates the required rheology capabilities in terms of the science requirements:

sample cell geometry:			
cone angle	0.15	radians	
plate radius	7.5	cm	
stiff foam (dry with small bubbles):			
surface tension	30	ergs/cm2	(typical)
bubble diameter	0.003	cm	(30μm)
shear modulus	10000	dynes/cm2	(surface tension/diameter)
yield strain	0.01		(typical)
yield stress	100	dynes/cm2	(modulus*yieldstrain)
angular position resolution = cone angle*strain resolution			
strain resolution	0.0001		(yield strain/100)
angular resolution	0.000015	radians	
	15	μradians	
speed range: rpm=strainrate*coneangle*(1/2π)*(60s/min)			
max strainrate	100	1/s	(10*1/duration of 0.1s)
min strainrate	0.001	1/s	(1000s=16min >>>> 1hour run)
max speed	143	rpm	(never need to go faster)
min speed	0.0014	rpm	(cannot reasonably go slower)
torque=stress*(2π/3)(R^3)(cos^2[coneangle])			
max stress	10000	dynes/cm2	(yieldstress*100)
max torque	8.6E+6	dyne-cm	
"	0.86	N-m	
min stress	0.001	dynes/cm2	(0.001*modulus*strainresolution)
min torque	0.86	dyne-cm	
"	0.086	μN-m	

The measurement capabilities of the commercial rheometer used by the PI [Paar-Physica UDS-200 Universal Dynamic Spectrometer] should thus suffice::

- angular position resolution: 1 μrad
- speed range: 10^{-5}–3000 rpm
- frequency range: 10^{-4}–100 Hz
- torque range: 0.5 μNm–150 mNm
- torque resolution: 0.01μNm
- axial stiffness: 49 N/μm
- axial position resolution: 1 μm

This instrument is of the "controlled stress" type, but with a very sophisticated feedback system between position measurement and applied torque so that it can be operated reliably in a "controlled strain" mode. The heart of the design is a brushless air-bearing motor for which the position is measured by optical encoders and for which the relation between current and torque is precisely calibrated. Besides elegance and simplicity of concept, the key advantage is that all rheological instrumentation exists only on the rotating tool; this simplification leaves the fixed tool and measurement chamber open for accommodation of optical diagnostics as well as loading

and cleaning operations. The cost is sophistication in electronics and software, plus a source of clean dry air at regulated pressure for the air bearing motor.

4.5 Diffusing-Light Spectroscopy Requirements

In this diagnostic, a laser beam is directed onto the sample at specified radial distance. The incident photons scatter so strongly from the gas-bubble interfaces within the foam that no unscattered/ballistic beam emerges from the opposite side. Instead, scattered photons execute a random walk via a series of scattering events until exiting from one side or the other. These diffusely transmitted or backscattered photons emerge over a broad area and are sprayed over all 2π directions away from the interface.

4.5.1 Illumination & Detection Geometry

To analyze data it is critical that the distribution of path lengths be calculable via diffusion and more sophisticated theories of photon transport. It is therefore crucial that the illumination and detection geometry be well-specified as either plane-in/plane-out or point-in/point-out. The former is equivalent to both plane-in/point-out and point-in/plane-out, and preferred for both simplicity and efficiency [49]. Thus, an effective plane-in/plane-out geometry shall be achieved via actual point-in illumination and plane-out detection, as specified further below.

4.5.2 Laser

The laser requirements can most likely be met with a commercial photodiode laser:

- visible wavelength, negligible absorption in surfactant solution
- single mode/single frequency cw operation
- coherence length > 10 m
- intensity stabilized against drifts and fluctuations
- power sufficient to obtain 1 MHz count rates in thickest samples
- polarization not critical
- beam spot of 1–2 mm diameter, no stray light outside spot

4.5.3 Light Collection

The diffusely transmitted and backscattered light at each DWS station shall be collected with a GRIN lens mounted to a single-mode optical fiber. The acceptance angle and sample-lens distance shall be sufficiently great so as not to discriminate against emerging photons according to *where* on the sample face they happen to emerge; this is crucial for obtaining a plane-out detection geometry. The sample-lens distance and GRIN lens diameter shall be optimized for collecting the maximum feasible solid angle of emerging photons. Stops and black paint shall be employed to prevent photons from one radial illumination distance from being collected by the detector for another radial illumination distance. The fiber length shall be short enough that reignition due to reflected photons occurs during the detector deadtime.

4.5.4 Detector

The fiber optic shall be coupled efficiently into an avalanche photodiode complete with amplification/discrimination electronics for photon-counting operation: photon in, TTL pulse out. Specifications shall meet or exceed those in typical dynamic light scattering apparatus, eg deadtime < 40 ns, quantum efficiency >50%, maximum count rate better than 10 MHz.

4.5.5 Correlator

The TTL pulses emerging from the detector circuitry shall be fed into a digital correlator for computation of both the average intensity <I> and the temporal autocorrelation function <I(0)I(t)>. Very fast dynamics are not expected, so the usual trick of splitting the optical fiber into two detectors and crosscorrelating to eliminate reignition and deadtime effects will probably not be required. In this case, the shortest sampling time need not be shorter than the deadtime of the detector. Commercial correlators sold by ALV, Brookhaven, or Flexible Instruments should suffice. Of these, Flexible Instruments is preferred because it alone is 100% efficient in processing the entire input signal and requires no user adjustments in response to changes in dynamics or light level.

4.6 Video Microscopy Requirements

Gas bubbles residing at the inner surface of the sidewall shall be imaged with a suitable microscope, and recorded live to videotape with a CCD camera, according to the following specifications:

4.6.1 Illumination

Illumination of surface bubbles within the field of view shall be with diffusely transmitted light. This is required to achieve contrast at the bubble edges via small-angle Fresnel reflection, as done for the photograph in Ref. [29]. To accomplish this, light from an incandescent bulb or LED shall be introduced just outside and around the field of view.

4.6.2 Imaging Optics

The magnification shall be variable such that the bubble size distribution may be estimated throughout the coarsening process, as the average diameter grows from the initial value of 10–30 μm up to about 500 μm. For the field of view to be 5–10 bubbles across, it must thus vary between about 100 μm and 5 mm across. The resolution shall be better than 1% of the field of view. The depth of field shall be no deeper than 20 μm. The image plane shall be located roughly one average bubble radius in from the sidewall, and it shall be possible to adjust the focus slightly. A calibrated reticule shall be superimposed at each magnification.

4.6.3 CCD Camera and Video Recording

The camera shall have at least 500x500 pixels and shall permit the observed gray scale to be stretched from black to white. Digital recording of the video signal should not be necessary; tape should suffice. The rate of recording shall be no slower than 10 frames/sec; standard video rates are preferred. The recording shall be provided with a time-stamp indicating the foam age.

4.7 Vibration and G-Jitter

The vibration control and measurement requirements are similar to those for flight experiments on colloids (PHASE and PCS), but more stringent because bubbles are larger than colloidal particles and because they have a greater density mismatch with the suspending liquid. In general, dc acceleration and low frequency jitter are most important to minimize.

As an order of magnitude estimate regarding acceleration-induced drainage, we may equate the maximum inertial force, mg, to the Stokes drag, $6\pi\eta RV$, and require that the drift during one oscillation period, V/ν, be much less than the bubble radius. Thus, the allowed amplitude g of acceleration at frequency ν must be restricted to

$$g/\nu \ll \frac{9\eta}{2\Delta\rho R}.$$

As an upper limit, the restriction for R=500μm gas bubbles in water is then

$$g/\nu \ll 1\frac{\mathrm{cm/s^2}}{\mathrm{Hz}} = 0.001\frac{g_{\mathrm{earth}}}{\mathrm{Hz}},$$

which gives the allowed duration of a $10^{-2}g_{\mathrm{earth}}$ maneuvering impulse as less than 0.1 seconds. Note, however, that this is an overestimate for several reasons. First, the actual drag is greater than the Stokes value because the bubbles are packed together, even in a very wet foam, and since there are additional loss mechanisms associated with the surfactants. Second, the above calculation ignores the hydrodynamic self-interaction, which will again increase the drag, especially at higher frequencies. Third, very gentle steady drainage in dry foams can occur by permeation without altering the bubble packing structure and without changing the liquid:gas ratio except at the sample boundaries.

As an order of magnitude estimate regarding acceleration-induced rearrangements, we may require that the inertial stress, mg/R^2, be much less than the yield stress, which is of order σ/R for dry foams. Thus, the allowed acceleration must be restricted to

$$g \ll \frac{3\sigma}{4\pi\Delta\rho R^2}.$$

As an upper limit for dry foams, the restriction for R=500μm gas bubbles in water is then $g \ll 3000\ \mathrm{cm/s^2} = 3g_{\mathrm{earth}}$. If this is exceeded, then the bubbles will rearrange. For wet foams, the yield stress decreases toward zero as $(\phi - \phi_c)^{\alpha}$ and the criterion becomes more stringent. Assuming α=1, as suggested by experiments on emulsions [21], the requirement becomes $g \ll 0.01g_{\mathrm{earth}}$ for $\phi - \phi_c = 10^{-2}$. Assuming α=1/2, as suggested by simulations [111,81,58], the requirement becomes $g \ll 0.01g_{\mathrm{earth}}$ for $\phi - \phi_c = 10^{-4}$. These numbers imply that acceleration-induce drainage will always be more important than acceleration-induced rearrangements and that the latter will not appreciably limit how close the melting point can be approached.

4.8 Astronaut Involvement and Experimental Activation

Astronauts will be needed to produce foams, load them into the sample cell, check visually for gross inhomogeneities, start the data collection software, and clean out the cell at the end of the run. For the video microscopy, they may also be needed to adjust the focus, change objectives, and load/unload/store videotapes.

4.9 Telepresence

For every foam loaded satisfactorily, it is anticipated that the *same* battery of standard rheology, DWS, and video diagnostics will be run as the sample ages. These are designed to capture the full range of behavior and should not need modification in response to the behavior of the sample. Nevertheless, it may be useful for the PI to be able to alter the sample and diagnostic matrices in response to the results of previous runs.

4.10 Postflight Data Deliverables

- raw data –time stamped with foam age– for DWS, rheology, and video diagnostics
- sealed volumetric foam samples for liquid content determination/verification
- base surfactant solution for ancillary measurements discussed in 4.2

4.11 Success Criteria

success	***accomplishment***
100%	complete DWS, rheology, and video diagnostics on sequence of volume fractions up to and beyond the melting point, as a function of time=bubble size; all repeated for several base solutions
90%	as above, but only one base solution
75%	few volume fractions, incomplete DWS or video diagnostics, or measured only for a total duration shorter than that needed for coarsening to produce a x10 increase in bubble diameter
<50%	poor quality samples, or incomplete rheology diagnostics

success criteria

5.0 APPENDICES

5.1 Foam Applications and Occurrences

Everyday Life:
- detergents
- foods (ice cream, meringue, beer, cappuccino, ...)
- cosmetics (shampoo, mousse, shaving cream, tooth paste, ...)

Unique Applications:
- firefighting
- isolating toxic materials
- delivering/spreading chemicals
- physical and chemical separations
- oil recovery
- cellular solids

Undesirable Occurrences:
- mechanical agitation of multicomponent liquid
- pulp and paper industry
- paint and coating industry
- textile industry
- leather industry
- adhesives industry
- polymer industry
- food processing
- metal treatment
- waste water treatment
- polluted natural waters

$\Rightarrow$ important in everyday, industrial, research, and environmental settings

$\Rightarrow$ need to control mechanical and stability properties

$\Rightarrow$ currently accomplished imperfectly via empirical trial & error

$\Rightarrow$ must understand microscopic structure and dynamics for rational guidance

6.0 REFERENCES

[1] J. J. Bikerman, *Foams* (Springer-Verlag, New York, 1973).

[2] D. Weaire and N. Rivier, "Soap, cells and statistics - random patterns in two dimensions," Contemp. Phys. **25**, 55 (1984).

[3] A. M. Kraynik, "Foam flows," Ann. Rev. Fluid Mech. **20**, 325-357 (1988).

[4] J. H. Aubert, A. M. Kraynik, and P. B. Rand, "Aqueous foams," Sci. Am. **254**, 74-82 (1989).

[5] A. J. Wilson, ed., *Foams: Physics, Chemistry and Structure.* Springer Series in Applied Biology , (Springer-Verlag, New York, 1989).

[6] D. J. Durian and D. A. Weitz, "Foams," in *Kirk-Othmer Encyclopedia of Chemical Technology*, 4 ed., edited by J.I. Kroschwitz (Wiley, New York, 1994), Vol. 11, p. 783-805.

[7] R. K. Prud'homme and S. A. Khan, ed., *Foams: Theory, Measurement, and Application.* Surfactant Science Series **57**, (Marcel Dekker, NY, 1996).

[8] K. J. Mysels, K. Shinoda, and S. Frankel, *Soap Films, Studies of Their Thinning and a Bibliography* (Pergamon Press, New York, 1959).

[9] I. B. Ivanov, ed., *Thin Liquid Films: Fundamentals and Applications.* Surfactant Science Series **29**, (Marcel Dekker, Inc., New York, 1988).

[10] M. J. Rosen, *Surfactants and Interfacial Phenomena*, 2nd ed. (John Wiley & Sons, New York, 1989).

[11] A. W. Adamson, *Physical Chemistry of Surfaces*, 5th ed. (John Wiley & Sons, New York, 1990).

[12] J. N. Israelachvili, *Intermolecular and Surface Forces*, 2nd ed. (Academic Press, San Diego, 1991).

[13] C. Isenberg, *The Science of Soap Films and Soap Bubbles* (Dover Publications, New York, 1992).

[14] G. R. Assar and R. W. Burley, "Hydrodynamics of foam flow in pipes, capillary tubes, and porous media," in *Gas-Liquid Flows*, edited by N.P. Cheremisinoff (Gulf Publishing Company, Houston, 1986), Vol. 3, p. 26-42.

[15] H. C. Cheng and T. E. Natan, "Measurement and physical properties of foam," in *Gas-Liquid Flows*, edited by N.P. Cheremisinoff (Gulf Publishing Company, Houston, 1986), Vol. 3, p. 3-25.

[16] J. P. Heller and M. S. Kuntamukkula, "Critical review of the foam rheology literature," Ind. Eng. Chem. Res. **26**, 318-325 (1987).

[17] D. M. A. Buzza, C. Y. D. Lu, and M. E. Cates, "Linear shear rheology of incompressible foams," J. de Phys. II **5**, 37-52 (1995).

[18] H. M. Princen, "Rheology of foams and highly concentrated emulsions. II. Experimental study of the yield stress and wall effects for concentrated oil-in-water emulsions," J. Coll. I. Sci. **105**, 150-171 (1985).

[19] H. M. Princen and A. D. Kiss, "Rheology of foams and highly concentrated emulsions. III. Static shear modulus," J. Coll. I. Sci. **112**, 427-437 (1986).

[20] S. A. Khan, C. A. Schnepper, and R. C. Armstrong, "Foam Rheology: III. Measurement of shear flow properties," J. Rheology **32**, 69-92 (1989).

[21] T. G. Mason, J. Bibette, and D. A. Weitz, "Elasticity of compressed emulsions," Phys. Rev. Lett. **75**, 2051-2054 (1995).

[22] R. Bruinsma, "Theory of hydrodynamic convection in soap films," Physica A **216**, 59-76 (1995).

[23] G. Verbist, D. Weaire, and A. M. Kraynik, "The foam drainage equation," Journal of Physics: Condensed Matter **8**, 3715-3731 (1996).

[24] J. A. Glazier and D. Weaire, "The kinetics of cellular patterns," J. Phys.: Condens. Matter **4**, 1867-1894 (1992).

[25] J. Stavans, "The evolution of cellular structures," Rep. Prog. Phys. **56**, 733-789 (1993).

[26] J. A. Glazier, S. P. Gross, and J. Stavans, "Dynamics of two-dimensional soap froths," Phys. Rev. A **36**, 306-316 (1987).

[27] K. J. Stine, S. A. Rauseo, B. G. Moore, J. A. Wise, and C. M. Knobler, "Evolution of foam structures in Langmuir monolayers of pentadecanoic acid," Phys. Rev. A **41**, 6884-6892 (1990).

[28] J. Stavans, "Temporal evolution of two-dimensional drained soap froths," Phys. Rev. A **42**, 5049-5051 (1990).

[29] D. J. Durian, D. A. Weitz, and D. J. Pine, "Scaling behavior in shaving cream," Phys. Rev. A **44**, R7902-R7905 (1991).

[30] N. O. Clark, "The electrical conductivity of foam," Trans. Faraday Soc. **44**, 13-15 (1948).

[31] A. K. Agnihotri and R. Lemlich, "Electrical conductivity and the distribution of liquid in polydedral foam," J. Coll. I. Sci. **84**, 42-46 (1981).

[32] R. Phelan, D. Weaire, E. A. J. F. Peters, and G. Verbist, "The conductivity of a foam," Journal of Physics: Condensed Matter **8**, L475-482 (1996).

[33] G. Nishioka and S. Ross, "A new method and apparatus for measuring foam stability," J. Coll. I. Sci. **81**, 1-7 (1981).

[34] A. J. Wilson, "Cryo-microscopical methods for the investigation of foam structure," in *Foams: Physics, Chemistry, and Structure*, edited by A.J. Wilson (Springer-Verlag, New York, 1989), p. 69-88.

[35] C. G. J. Bisperink, A. D. Ronteltap, and A. Prins, "Bubble size distribution in foams," Adv. Coll. I. Sci. **38**, 13 (1992).

[36] C. P. Gonatas, J. S. Leigh, A. G. Yodh, J. A. Glazier, and B. Prause, "Magnetic resonance images of coarsening inside a foam," Phys. Rev. Lett. **75**, 573-576 (1995).

[37] B. A. Prause, J. A. Glazier, S. J. Gravina, and C. D. Montemagno, "Three-dimensional magnetic resonance imaging of a liquid foam," Journal of Physics: Condensed Matter **7**, L511-516 (1995).

[38] K. Kose, "3D NMR imaging of foam structures," Journal of Magnetic Resonance, Series A **118**, 195-201 (1996).

[39] M. G. Reed, C. V. Howard, and C. G. Shelton, "Confocal imaging and second-order stereological analysis of a liquid foam," Journal of Microscopy **185 pt.3**, 313-320 (1997).

[40] D. A. Weitz, J. X. Zhu, D. J. Durian, H. Gang, and D. J. Pine, "Diffusing-wave spectroscopy: The technique and some applications," Physica Scripta **49B**, 610-626 (1993).

[41] D. J. Durian, "Relaxation in aqueous foams," Bull. Mat. Res. Soc. **19**, 20-23 (1994).

[42] D. J. Durian, "Fast, nonevolutionary dynamics in foams," Current Opinion in Colloid and Interface Science **2**, 615-621 (1997).

[43] M. Tabor, J. J. Chae, G. D. Burnett, and D. J. Durian, "The structure and dynamics of foams," Nonlinear Science Today (1998).

[44] D. J. Durian, D. A. Weitz, and D. J. Pine, "Multiple light scattering probes of foam structure and dynamics," Science **252**, 686-688 (1991).

[45] A. D. Gopal and D. J. Durian, "Nonlinear bubble dynamics in a slowly driven foam," Phys. Rev. Lett. **75**, 2610-2613 (1995).

[46] A. D. Gopal and D. J. Durian, "Fast thermal dynamics in aqueous foams," J. Opt. Soc. Am. A **14**, 150-155 (1997).

[47] D. J. Durian, "The influence of boundary reflection and refraction on diffusive photon transport," Phys. Rev. E **50**, 857-866 (1994).

[48] D. J. Durian, "Accuracy of diffusing-wave spectroscopy theories," Phys. Rev. E **51**, 3350-3358 (1995).

[49] D. J. Durian, "Penetration depth for diffusing-wave spectroscopy," Appl. Opt. **34**, 7100-7105 (1995).

[50] M. U. Vera and D. J. Durian, "The angular distribution of diffusely transmitted light," Phys. Rev. E **53**, 3215-3224 (1996).

[51] M. U. Vera, P.-A. Lemieux, and D. J. Durian, "The angular distribution of diffusely backscattered light," J. Opt. Soc. Am. A **14**, 2800-2808 (1997).

[52] D. J. Durian, "Two-stream theory of diffusing-light spectroscopies," Physica A **229**, 218-235 (1996).

[53] D. J. Durian and J. Rudnick, "Photon migration at short times and distances, and in cases of strong absorption," J. Opt. Soc. Am. A **14**, 235-245 (1997).

[54] P.-A. Lemieux, M. U. Vera, and D. J. Durian, "Diffusing-light spectroscopies outside the diffusive limit: the role of ballistic transport and anisotropic scattering," Phys. Rev. E **57**, 4498-4515 (1998).

[55] S. S. Park and D. J. Durian, "Viscous and elastic fingering instabilities in foam," Phys. Rev. Lett. **72**, 3347-3350 (1994).

[56] A. D. Gopal and D. J. Durian, "Crossover from discrete rearrangements to homogeneous shear deformation in a flowing foam," preprint (1998).

[57] D. J. Durian, "Foam mechanics at the bubble scale," Phys. Rev. Lett. **75**, 4780-4783 (1995).

[58] D. J. Durian, "Bubble-scale model of foam mechanics: Melting, nonlinear behavior, and avalanches," Phys. Rev. E **55**, 1739-1751 (1997).

[59] P. D. Kaplan, A. D. Dinsmore, A. G. Yodh, and D. J. Pine, "Diffuse-transmission spectroscopy: A structural probe of opaque colloidal mixtures," Phys. Rev. E **50**, 4827-4835 (1994).

[60] G. Maret and P. E. Wolf, "Multiple light scattering from disordered media. The effect of Brownian motion of scatterers.," Z. Phys. B **65**, 409-413 (1987).

[61] D. J. Pine, D. A. Weitz, P. M. Chaikin, and E. Herbolzheimer, "Diffusing-wave spectroscopy," Phys. Rev. Lett. **60**, 1134-1137 (1988).

[62] M. J. Stephen, "Temporal fluctuations in wave propagation in random media," Phys. Rev. B **37**, 1-5 (1988).

[63] D. A. Weitz and D. J. Pine, "Diffusing-wave spectroscopy," in *Dynamic Light Scattering: The Method and some Applications*, edited by W. Brown (Claredon Press, Oxford, 1993), p. 652-720.

[64] X.-l. Wu, D. J. Pine, P. M. Chaikin, J. S. Huang, and D. A. Weitz, "Diffusing-wave spectroscopy in a shear flow," J. Opt. Soc. Am. B **7**, 15-20 (1990).

[65] Y. Kwon and A. I. Leonov, "Remarks on orthogonal superposition of small amplitude oscillations on steady shear flow," Rheologica Acta **32**, 108-112 (1993).

[66] P. Moldenaers and J. Mewis, "On the nature of viscoelasticity in polymeric liquid crystals," J. Rheol. **37**, 367-380 (1993).

[67] P. Moldenaers, H. Yanase, J. Mewis, G. G. Fuller, C. S. Lee, and J. J. Magda, "Flow-induced concentration fluctuations in polymer solutions: structure/property relationships," Rheologica Acta **32**, 1-8 (1993).

[68] J. Zeegers, D. van den Ende, C. Blom, E. G. Altena, G. J. Beukema, and J. Mellema, "A sensitive dynamic viscometer for measuring the complex shear modulus in a steady shear flow using the method of orthogonal superposition," Rheologica Acta **34**, 606-621 (1995).

[69] B. A. De L. Costello, "Parallel superposition rheology of polyethylene as a function of temperature," Journal of Non-Newtonian Fluid Mechanics **68**, 303-309 (1997).

[70] J. Vermant, P. Moldenaers, J. Mewis, M. Ellis, and R. Garritano, "Orthogonal superposition measurements using a rheometer equipped with a force rebalanced transducer," Review of Scientific Instruments **68**, 4090-4096 (1997).

[71] C. W. Macosko, *Rheology Principles, Measurements, and Applications* (VCH Publishers, Inc., New York, 1994).

[72] L. J. Gibson and M. F. Ashby, *Cellular Solids*, 2 ed. (Cambridge, 1997).

[73] M. U. Vera and D. J. Durian, "Convection and size segregation in foams continuously wetted from above," unpublished (1998).

[74] H. M. Princen, "Highly concentrated emulsions. I. Cylindrical systems," J. Coll. I. Sci. **71**, 55-66 (1979).

[75] H. M. Princen, "Rheology of foams and highly concentrated emulsions. I. Elastic properties and yield stress of a cylindrical model system," J. Col. I. Sci. **91**, 160-175 (1983).

[76] R. K. Prud'homme, "Foam flow," presented at Ann. Meet. Soc. Rheol., Louisville KY. (1981).

[77] D. Weaire and J. P. Kermode, "Computer simulation of a two-dimensional soap froth I. Method and motivation," Phil. Mag. B **48**, 245-259 (1983).

[78] F. Bolton and D. Weaire, "The effects of Plateau borders in the two-dimensional soap froth. I. Decoration lemma and diffusion theorem," Phil. Mag. B **63**, 795-809 (1991).

[79] F. Bolton and D. Weaire, "The effects of Plateau borders in the two-dimensional soap froth. II. General simulation and analysis of rigidity loss transition," Philosophical Magazine B **65**, 473-487 (1992).

[80] T. Herdtle and H. Aref, "Numerical experiments on two-dimensional foam," J. Fluid Mech. **241**, 233-260 (1992).

[81] S. Hutzler, D. Weaire, and F. Bolton, "The effects of plateau borders in the two-dimensional soap froth. III. Further results," Philosophical Magazine B **71**, 277-289 (1995).

[82] K. A. Brakke, “The surface evolver,” Exp. Math. **1**, 141-165 (1992).

[83] D. Weaire and R. Phelan, “A counter-example to Kelvin's conjecture on minimal surfaces,” Phil. Mag. Lett. **69**, 107-110 (1994).

[84] D. A. Reinelt and A. M. Kraynik, “Simple shearing flow of a dry Kelvin soap foam,” J. Fluid Mech **331**, 327-343 (1996).

[85] A. M. Kraynik and D. A. Reinelt, “The linear elastic behavior of dry soap foams,” J. Coll. I. Sci **181**, 511-520 (1996).

[86] A. M. Kraynik, “personal communication,” (1997).

[87] K. Kawasaki, T. Okuzono, and T. Nagai, “Mechanical and flow behavior of two-dimensional foams,” J. Mech. Behav. Mat. **4**, 51-60 (1992).

[88] T. Okuzono and K. Kawasaki, “Rheology of random foams,” J. Rheol. **37**, 571-586 (1993).

[89] T. Okuzono and K. Kawasaki, “Intermittent flow behavior of random foams: a computer experiment on foam rheology,” Phys. Rev. E **51**, 1246-1253 (1995).

[90] W. Schwartz and H. M. Princen, J. Coll. I. Sci. **118**, 201 (1987).

[91] D. A. Reinelt and A. M. Kraynik, “Viscous effects in the rheology of foams and concentrated emulsions,” J. Coll. I. Sci. **132**, 491-503 (1989).

[92] D. A. Reinelt and A. M. Kraynik, “On the shearing flow of foams and concentrated emulsions,” J. Fluid Mech. **215**, 431-455 (1990).

[93] S. A. Langer and A. J. Liu, “Effect of random packing on stress relaxation in foam,” J. Phys. Chem. B **101**, 8667-8671 (1997).

[94] S. A. Langer, S. Tewari, D. Schiemann, A. J. Liu, and D. J. Durian, “preprint,” (1998).

[95] D. C. Morse and T. A. Witten, “Droplet elasticity in weakly compressed emulsions,” Europhys. Lett. **22**, 549-555 (1993).

[96] M. D. Lacasse, G. S. Grest, and D. Levine, “Deformation of small compressed droplets,” Phys. Rev. E **54**, 5436-5446 (1996).

[97] M. D. Lacasse, G. S. Grest, D. Levine, T. G. Mason, and D. A. Weitz, “Model for the elasticity of compressed emulsions,” Phys. Rev. Lett. **76**, 3448-3451 (1996).

[98] T. G. Mason, M. D. Lacasse, G. S. Grest, D. Levine, J. Bibette, and D. A. Weitz, “Osmotic pressure and viscoelastic shear moduli of concentrated emulsions,” Phys. Rev. E **56**, 3150-3166 (1997).

[99] J. D. Goddard, A. M. Kraynik, and A. J. Liu, “personal communication,” (1997).

[100] P. M. Lovalenti and J. F. Brady, “The force on a bubble, drop, or particle in arbitrary time-dependent motion at small Reynolds number,” Physics of Fluids A (Fluid Dynamics) **5**, 2104-2116 (1993).

[101] M. R. Kennedy, C. Pozrikidis, and R. Skalak, “Motion and deformation of liquid drops, and the rheology of dilute emulsions in simple shear flow,” Computers & Fluids **23**, 251-278 (1994).

[102] X. Li, R. Charles, and C. Pozrikidis, “Simple shear flow of suspensions of liquid drops,” J. Fluid Mech. **320**, 395-416 (1996).

[103] Y. Yurkovetsky and J. F. Brady, "Statistical mechanics of bubbly liquids," Physics of Fluids **8**, 881-895 (1996).

[104] K. Sang-Yoon, A. S. Sangani, T. Heng-Kwong, and D. L. Koch, "Rheology of dense bubble suspensions," Physics of Fluids **9**, 1540-1561 (1997).

[105] L. Xiaofan and C. Pozrikidis, "The effect of surfactants on drop deformation and on the rheology of dilute emulsions in Stokes flow," J. Fluid Mech. **341**, 165-194 (1997).

[106] J. F. French and R. J. Fry, "A mechanical foam-generator for use in laboratories," J. Appl. Chem. **1**, 425-429 (1951).

[107] J. J. Kroll, "Foam generating apparatus and method," USA Patent No. 4,474,680 (1984).

[108] P. A. Kittle, "Method of providing a barrier between a substrate and the atmosphere and compositions therefore," USA Patent No. 4,874,641 (1989).

[109] P. A. Kittle, "Composition for providing a foam barrier between a substrate and the atmosphere and the method of use," USA Patent No. 5,215,786 (1993).

[110] P. A. Sanders, *Handbook of Aerosol Technology*, 2nd ed. (Van Nostrand Reinhold Company, New York, 1979).

[111] F. Bolton and D. Weaire, "Rigidity loss transition in a disordered 2D froth," Phys. Rev. Lett. **65**, 3449-3451 (1990).